Water Air Soil Pollut (2019) 230: 50
https://doi.org/10.1007/s11270-019-4104-2

Novel Crayfish Shell Biochar Nanocomposites Loaded with Ag-TiO_2 Nanoparticles Exhibit Robust Antibacterial Activity

Yifan Zeng · Yingwen Xue · Li Long · Jinpeng Yan

Received: 16 October 2018 / Accepted: 28 January 2019 / Published online: 6 February 2019

Abstract A fast sol-dipping-gel method was applied to load Ag and TiO_2 nanoparticles on the surface of crayfish shell biochar to make an inexpensive and novel nanocomposite. Tetra-n-butyl titanate ($Ti(OC_4H_9)_4$) and silver nitrate ($AgNO_3$) were used as the nanoparticle precursors. Crayfish shell was pyrolyzed to produce the biochar host. Paper-disk diffusion method was applied to measure antibacterial activities of the nanocomposites to *E. coli*. The maximum loading rate of TiO_2 and Ag nanoparticles on the biochar reached 7.54% and 3.20%, respectively. Results of long-term antibacterial effect experiment showed that the Ag-TiO_2-biochar had robust antibacterial activity and could be reused for multiple times. The inactivation of *E. coli* of initial concentration of 10^5 CFU/mL by Ag-TiO_2-biochar under solar light reached around 99% of sterilization ratio in 5 min. In addition, the antibacterial ability of the nanocomposite was better in light than that in dark due to the presence of TiO_2. Findings of this study suggest that the novel nanocomposite is a promising material for water treatment units and household water purifiers.

Y. Zeng · Y. Xue · L. Long · J. Yan
School of Civil Engineering, Wuhan University, Wuhan, China

Y. Xue (✉)
Engineering Research Center of Urban Disasters Prevention and Fire Rescue Technology of Hubei Province, Wuhan, China
e-mail: ywxue@whu.edu.cn

Keywords Biochar · Nanocomposites · Ag-TiO_2 nanoparticles · Antibacterial activity

1 Introduction

Nowadays, water pollution has caused great harm to humans all over the world. Pathogenic bacteria in drinking water may lead to the transmission of severe diseases. In many developing countries, pathogen-polluted water has caused a big amount of death and a highly efficient antibacterial and inexpensive material for water treatment is thus needed. Antibiotics, metal ions, quaternary ammonium compounds, silver nanoparticles (Ag-NPs) and titanium oxide nanoparticles (TiO_2-NPs) (Amin et al. 2009; Necula et al. 2011, 2012; Liu et al. 2013; Selvam et al. 2012), nanocomposite films (Liu et al. 2008; Yao et al. 2008; Mai et al. 2010), and nanocomposite membranes (Ma et al. 2009; Goei and Lim 2014) have been applied in daily life as effective antibacterial materials.

In recent years, titanium dioxide (TiO_2) has attracted great attention as an antibacterial material because of its low cost, low toxicity, high stability, and high efficiency (Damodar et al. 2009; Etacheri et al. 2015; Armelao et al. 2007; Morikawa et al. 2006; Tong et al. 2013; Huo et al. 2014; Albert et al. 2015). When illuminated with the sun light, TiO_2 can serve as a catalyst to generate free radicals ($^{\bullet}OH$ and $^{\bullet}O^{-}$) from O_2 and water:

$$TiO_2 + h\upsilon \rightarrow TiO_2(e^{\bullet} + h^{+}) \quad (1)$$

$$H_2O + TiO_2\ (h^{+}) \rightarrow TiO_2 + {}^{\bullet}OH + H^{+} \quad (2)$$

$$O_2 + TiO_2(e^{\bullet}) \rightarrow TiO_2 + {}^{\bullet}O^{-} \quad (3)$$

When TiO_2 is excited by the photon energy comparable to or greater than its band gap, electron-hole pair is generated and further procured strong redox reactions to produce radicals to bacteria.

Cheng et al. (Cheng et al. 2006) grafted gamma-aminopropyltriethoxysilane (APS) on TiO_2/Ag^+ nanoparticles to make a modified composite. Their characterization results showed that APS is chemically bonded to the surface of antibacterial TiO_2/Ag^+ nanoparticles. The bacteriostatic rates towards *E. coli* and Staphylococci were 93.29% and 96.73%, respectively. Akhavan (Akhavan 2009) prepared Ag-TiO_2/Ag/a-TiO_2 nanocomposite thin film photocatalysts and studied their lasting antibacterial activities. Their results showed that antibacterial activity of the nanocomposite film against *E. coli* bacteria is more effective in solar light than in dark. Furthermore, the antibacterial rate of Ag-TiO_2/Ag/a-TiO_2 photocatalysts reached 100% in 90 min. Liu et al. (Liu et al. 2012) prepared an antibacterial and photocatalytic PVC film by doping heteronanostructure of TiO_2 nanowire at Ag nanoparticles. TiO_2 nanowire with 50–60 nm in diameter and 0.1 mm in length was prepared by a hydrothermal method, and Ag nanoparticle about 5–10 nm in diameter was grafted on the surface of TiO_2 nanowire. The highest loading rate of TiO_2-Ag nanoparticles was 1.25%, and the maximum inhibitory rate of the materials reached about 97%.

It is well known that silver ion has extremely strong antibacterial effect and TiO_2 possesses excellent photocatalysis ability (Albert et al. 2015; Li et al. 2013; Perkas et al. 2013; Wei et al. 2015; Tan et al. 2009). When Ag and TiO_2 are made into nanoparticles, their antibacterial capacities increase a lot. However, some materials studied are complicated to prepare or the cost is too high to be made in large production. Furthermore, nanoparticles are easy to aggregate and settle in liquid, which would considerably reduce their antibacterial capacity. Besides, nanoparticles in solution are difficult to be collected due to their extremely small particle sizes. Therefore, studies are conducted to attach Ag and TiO_2 nanoparticles on carriers to optimize their ability.

In this study, a novel antibacterial nanocomposite was made to solve abovementioned problems with the following procedures: (1) crayfish shell, as an inexpensive and widely available biomaterial, was pyrolyzed to be a nanoparticle carrier, and Ag-TiO_2 nanoparticles were loaded on the biochar to produce a novel nanocomposite; (2) different loading methods were applied to increase the loading rate of Ag-TiO_2; and (3) *E. coli* bacteria were chosen to study the antibacterial activity of the nanocomposites, and the reutilization ability of the Ag-TiO_2-biochar was tested.

2 Experimental

2.1 Materials and Methods

All the chemical reagents of analytical grade were purchased from Sinopharm Chemical Reagent Co., Ltd. The crayfish shell was obtained from a seafood market (Wuhan, China). Deionized (DI) water was used to prepare all chemical solutions.

2.2 Preparation of Crayfish Shell Biochar

The crayfish shell was washed, and oven dried at 80 °C. It was then pyrolyzed in a quartz tube under N_2 flow at 450 °C for 2 h (Long et al. 2017). After the biochar was cooled to ambient temperature, it was ground in a mortar with a pestle and sieved to a uniform size of 1.5–2.5 mm. Finally, the ground biochar was washed with DI water, oven dried at 80 °C, and stored in a sealed container for the following loading process.

2.3 Loading of Ag-TiO_2 Nanoparticles on Biochar

The Ag-TiO_2 nanoparticle–coated crayfish shell biochar was prepared by a sol-dipping-gel method (Macwan et al. 2011; Choi et al. 2006; Lee et al. 2005) with TiO_2 and Ag nanoparticles loaded on the biochar sequentially. During the loading of TiO_2 nanoparticles, tetra-n-butyl titanate ($Ti(OC_4H_9)_4$) was used as the precursor. 68.7 mL $Ti(OC_4H_9)_4$ was dissolved in 117 mL ethanol and was stirred for 2 h (150 rpm) with a magnetic stirrer. While stirring, 3.33 mL HCl (35%) and 0.36 mL DI water were mixed and added to the solution drop by drop at an ambient temperature. Then, 6.20 mL acetyl acetone was slowly added to the sol. After 24 h, biochar was completely mixed with the sol and the mixture was sonicated for 10 min. The sol-coated biochar was dried for 2 h at 80 °C, and then calcined at 300 °C for 2 h with N_2 flow in the tubular furnace. Finally, the TiO_2-biochar was cooled to ambient temperature and stored in a sealed container for the next process.

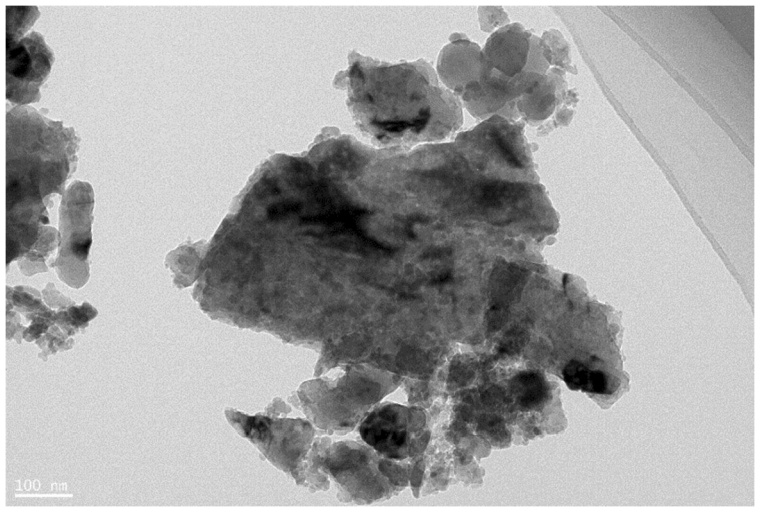

Fig. 1 TEM image of crayfish shell biochar

During the loading of Ag nanoparticles, TiO_2-biochar was added to 0.1 M $AgNO_3$ solution and the mixture was sonicated for 10 min. Then, the coated biochar was dried at 80 °C for 2 h and calcined at 450 °C for 2 h with N_2 flow in a tubular furnace. Finally, the Ag-TiO_2 nanoparticle–coated biochar was obtained and stored for the following experiment. At the meantime, TiO_2-biochar was made using the same method without loading Ag nanoparticles on the biochar. This kind of biochar was named Ag-TiO_2-biochar-2 in this article. Another type of Ag-TiO_2-biochar-1 was prepared by dipping biochar in two kinds of solution mentioned above successively; then, the biochar was calcined at 450 °C to load both Ag and TiO_2 nanoparticles at the same time.

2.4 Antibacterial Activity Test

The long-term antibacterial effect of the biochar, TiO_2-biochar, and two Ag-TiO_2-biochars was tested with paper-disk diffusion method. *Escherichia coli* (CMCC:44102) was selected as a bacterial model. Luria-Bertani (LB) medium was applied to grow and maintain the bacterial liquid cultures, and a solid medium was obtained by adding 2% agar into the liquid medium. Fifty milligrams of different biochar particles were uniformly dispersed on the filter paper disks (2 cm in diameter) and placed onto the agar plates with *E. coli* (3 mL, 10^5 colony forming units per mL). After incubation at 37 °C for 24 h, the diameters of the inhibition zones were measured.

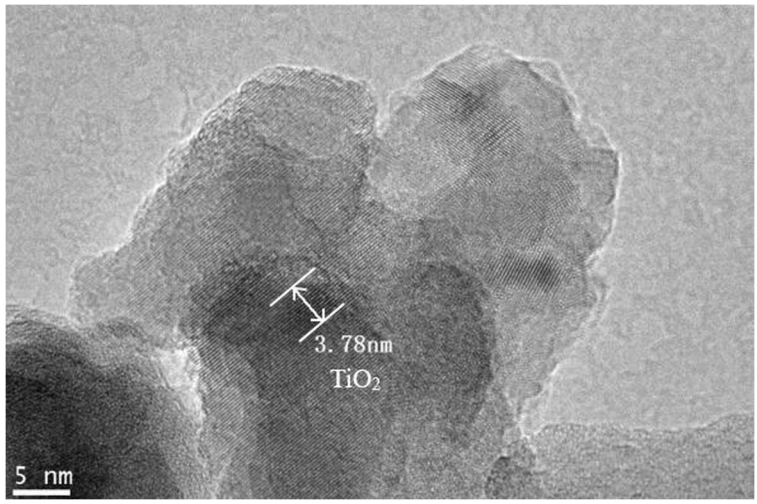

Fig. 2 TEM image of TiO_2-biochar

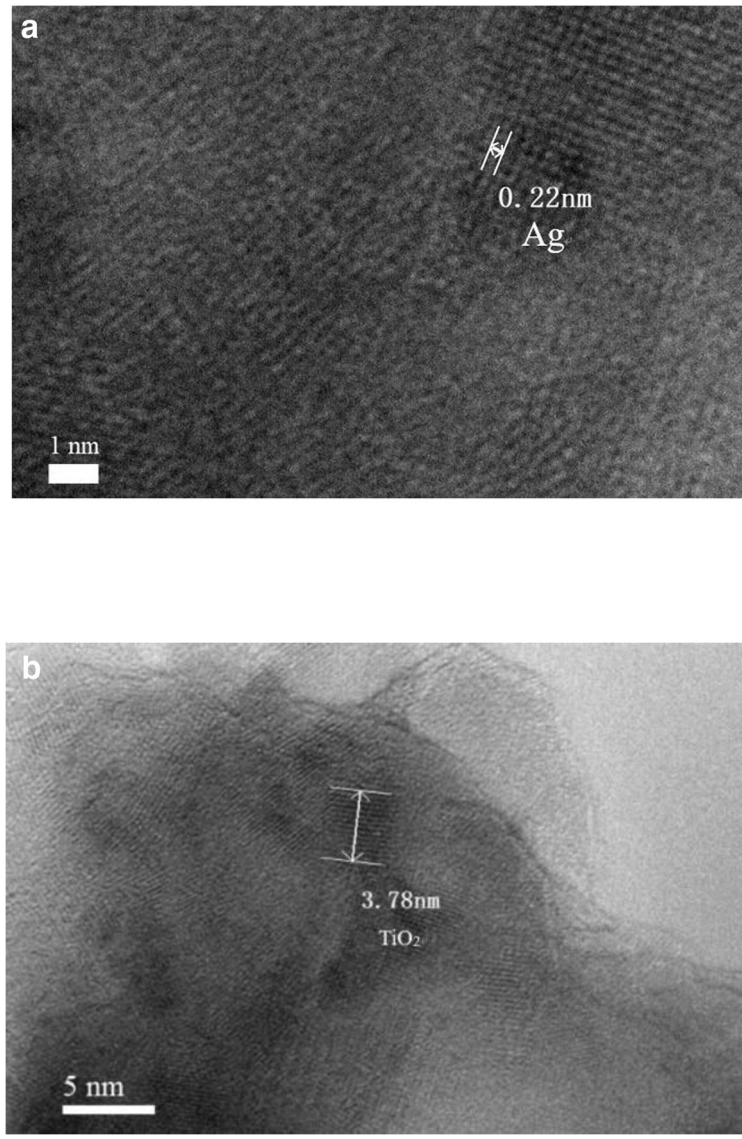

Fig. 3 TEM image of Ag-TiO_2-biochar

The short-term antibacterial properties of the Ag-TiO_2-biochar were tested by the plate-count method. The biochar was soaked in *E. coli* solution of 10^5 CFU/mL for 5 min. Then, 3 mL sterilized solution was spread on the agar plates and incubated at 37 °C for 24 h. The colonies of the *E. coli* were counted. Three parallel samples were used in the short-term experiment. The antibacterial rate, *R*, was calculated by the following formula (Chen et al. 2016):

$$R = \frac{C_0 - C}{C_0} \times 100\% \quad (4)$$

where C_0 and C are the average number of the bacterial colony before and after the sterilization, respectively. According to the National Standard of China (GB/T 4789.2–2010), $R \geq 99\%$ means that the sample has strong antibacterial property and $R \geq 90\%$ means that the sample has antibacterial property.

2.5 Characterization

The surface morphology of the samples was acquired by transmission electron microscope (TEM, JEM-2100, JEOL, Japan) at an accelerating voltage of 200 kV. To detect crystalline minerals on the samples, a computer controlled X-ray diffractometer (XRD, PANalytical, X'Pert Pro, Netherlands) was applied to the samples. The elemental analysis was performed using an

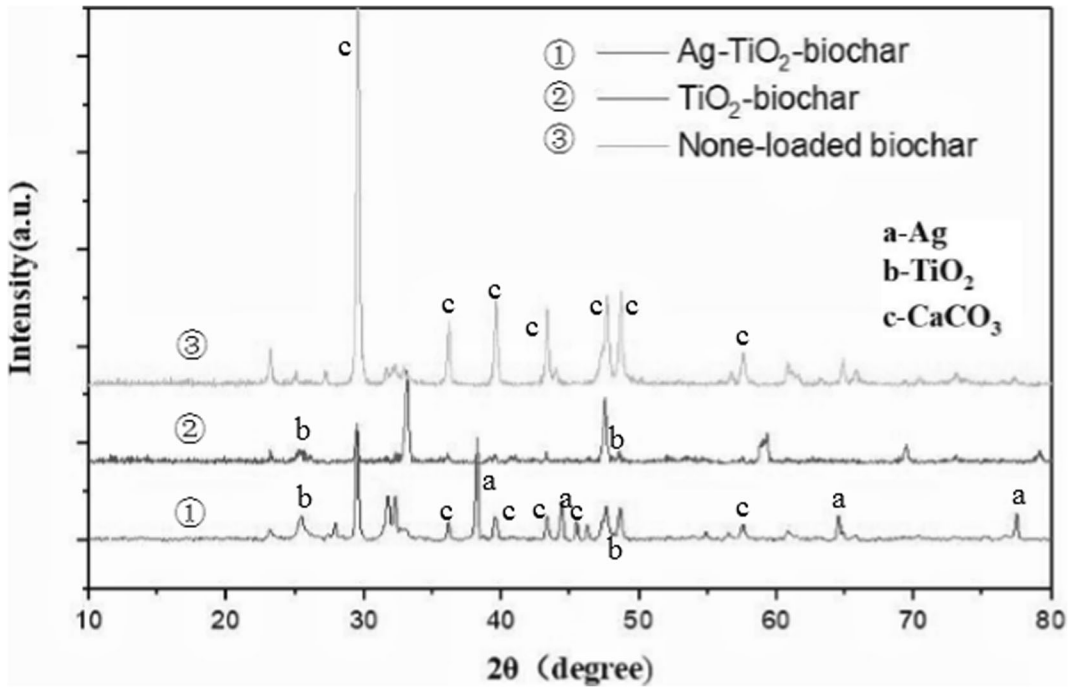

Fig. 4 XRD image of three kinds of biochar

inductively coupled plasma-atomic emission spectrometer (ICP-AES, IRIS Intrepid II XSP, USA).

3 Results and Discussion

3.1 Biochar Characterization

Figure 1 displays the TEM image of crayfish shell biochar. It can be observed that the crayfish shell biochar possessed rough surface and multi-layered structure, showing porous structure, which would provide enormous area for the loading of nanoparticles. Meanwhile, crayfish biochar possessed strong structure stability, which can bear home water supply pressure in a long time, increasing the reusability of the nanocomposites.

Figure 2 displays the TEM image of crayfish shell biochar coated with TiO_2 nanoparticles. It can be observed that TiO_2 was distributed on the surface of the crayfish shell biochar.

Figure 3a and b display the TEM image of crayfish shell biochar coated with TiO_2 and Ag nanoparticles. It can be observed that both TiO_2 and Ag nanoparticles were distributed on the surface. There was no obvious aggregation of nanoparticles on the surface because the large surface area and porous structure of the biochar facilitated the distribution of the nanoparticles.

Figure 4 displays the XRD spectra of none-loaded biochar, TiO_2-biochar, and Ag-TiO_2-biochar. The crystalline nature of the none-loaded biochar clearly changed after the loading, confirming the loading of Ag and TiO_2 nanoparticles. After loading, the XRD pattern of Ag-TiO_2-biochar showed several new peaks, which can be assigned to cubic phase of Ag (a) and anatase TiO_2 (b). As $CaCO_3$(c) was the main component of crayfish shell biochar, its peak was also identified.

According to the results of elemental analysis by ICP-AES, the loading capacity of TiO_2 and Ag nanoparticles on 20 mg the biochar produced with Ag and TiO_2 nanoparticles loaded simultaneously were 1.487 mg and 0.552 mg, and the loading rate were 7.44% and 2.76%, respectively. The loading capacity of TiO_2 and Ag nanoparticles on the biochar with nanoparticles loaded sequentially were 1.508 mg and 0.64 mg, with loading rate of 7.54% and 3.20%, respectively. Evidently, the loading rate of the sequential-loading method was higher than that of the simultaneous-loading method, especially for Ag loading rate. The results indicate that sequential loading may be an effective method to reduce the loss of nanoparticles during the production of nanocomposites.

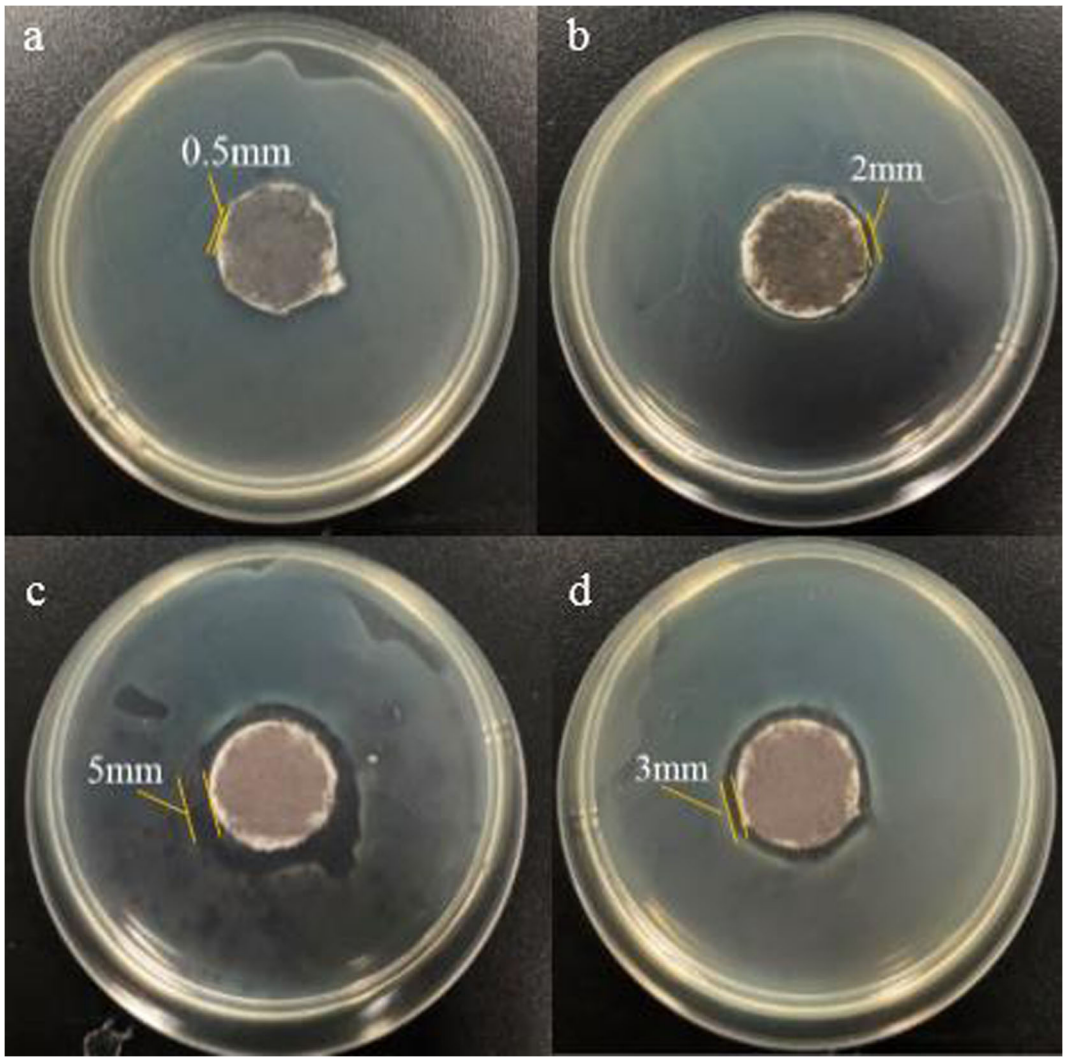

Fig. 5 Incubation zone of TiO_2-biochar (**a**), Ag-TiO_2-biochar-1 (**b**), Ag-TiO_2-biochar-2 (**c**), Ag-TiO_2-biochar-2 (aphotic) (**d**)

3.2 Antibacterial Effect

The long-term antibacterial activities of crayfish shell biochar, TiO_2-biochar, and Ag-TiO_2-biochar were evaluated by the disk diffusion method. The antibacterial performances of all the materials are displayed in Fig. 5. Obviously, crayfish shell biochar did not possess the antibacterial ability and did not show any inhibition zone. After the biochar was loaded with TiO_2 nanoparticles, it showed some antibacterial effect with a ca. 0.5 mm inhibition zone (Fig. 5a), which is attributed to the antibacterial activity of TiO_2 nanoparticles. With Ag nanoparticles loaded on TiO_2-biochar, the biochar presented robust antibacterial activity. The inhibition zone of biochar with Ag and TiO_2 nanoparticles loaded simultaneously (Ag-TiO_2-biochar-1) was ca. 2 mm (Fig. 5b),

Table 1 Results of long-term antibacterial activities

Type of the composites	Crayfish biochar	TiO_2-biochar	Ag-TiO_2-biochar-1	Ag-TiO_2-biochar-2	Ag-TiO_2-biochar-2 (aphotic)
Width of the inhibition zone/mm	0	0.5	2.0	5.0	3.0

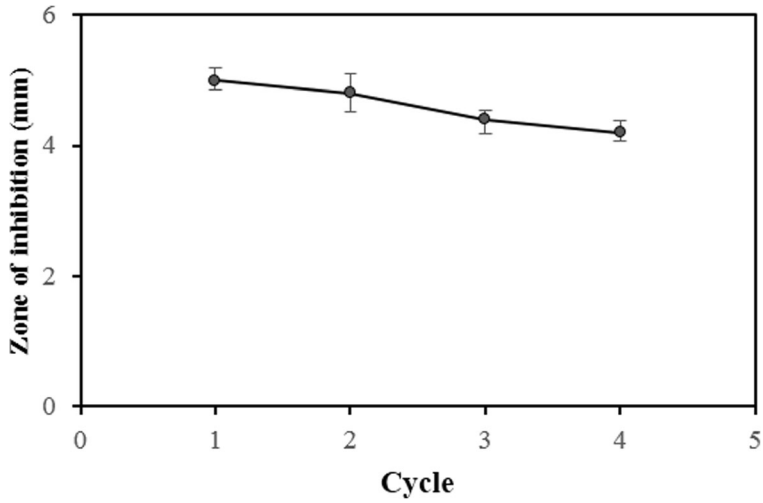

Fig. 6 Repeated use of Ag-TiO_2-biochar

while the inhibition zone of biochar with Ag and TiO_2 loaded sequentially (Ag-TiO_2-biochar-2) was ca. 5 mm (Fig. 5c). The greatly enhanced antibacterial activity of the Ag-TiO_2-biochar (compared with biochar and TiO_2-biochar) is clearly due to the loading of Ag nanoparticles. The inhibition zone of Ag-TiO_2-biochar-2 was much larger than that of Ag-TiO_2-biochar-1, which is consistent with the Ag and TiO_2 loading capacity listed in Table 1. In Fig. 5d, the culture medium with Ag-TiO_2-biochar-2 was put in an aphotic incubator and after incubation, the inhibition zone was ca. 3 mm. This probably can be attributed to the inhibition of TiO_2 activity in an aphotic environment (Li et al. 2011). The long-term antibacterial activity results are also shown in Table 1.

Figure 6 shows antibacterial behavior for repeated use of Ag-TiO_2-biochar-2. The antibacterial test was conducted for four times. The diameter of the zone of inhibition gradually decreased with the repeat, but the reduction was small. Meanwhile, the Ag and TiO_2 contents of the nanocomposite only reduced slightly during the antibacterial tests. These indicate that Ag-TiO_2-biochar possesses robust antibacterial activity and reusability.

Table 2 Antibacterial rate of the Ag-TiO2-biochar-2

Initial concentration/ CFU mL^{-1}	Concentration after sterilization/CFU mL^{-1}	Average antibacterial rate
1×10^5	12 18 10	$R \geq 99\%$

With the best antibacterial property, the Ag-TiO_2-biochar-2 was chosen to further evaluate its short-term antibacterial activity. The results are listed in Table 2. According to the National Standard of China (GB/T 4789.2-2010), Ag-TiO_2-biochar-2 had strong antibacterial property because its average antibacterial rate was larger than 99%.

4 Conclusions

A sol-dipping-gel method was developed to load Ag and TiO_2 nanoparticles on crayfish shell biochar. The sequential-loading method was better than the simultaneous-loading method and enhanced the loading rate of Ag and TiO_2 nanoparticles. The maximum loading rate of TiO_2 and Ag nanoparticles on the biochar reached 7.54% and 3.20%, respectively. The antibacterial activity test showed that the Ag-TiO_2-biochar possessed robust antibacterial activity and reusability. In addition, its sterilization rate in the short-term test was above 99%. With excellent antibacterial properties, the Ag-TiO_2-biochar shows great potential in environmental applications for disinfection of water, air, and solid surfaces.

Acknowledgements This work was partially supported by Wuhan Water Engineering and Technology Co. Ltd.

Funding Information This work was partially supported by the National "Twelfth Five-Year" Plan for Science and Technology Pillar Program [grant number 2015BAL01B02].

References

Akhavan, O. (2009). Lasting antibacterial activities of Ag-TiO2/Ag/a-TiO2 nanocomposite thin film photocatalysts under solar light irradiation. *Journal of Colloid and Interface Science, 336*(1), 117–124.

Albert, E., et al. (2015). Antibacterial properties of Ag–TiO2 composite sol–gel coatings. *RSC Advances, 5*(73), 59070–59081.

Amin, S. A., Pazouki, M., & Hosseinnia, A. (2009). Synthesis of TiO2–Ag nanocomposite with sol–gel method and investigation of its antibacterial activity against E. coli. *Powder Technology, 196*(3), 241–245.

Armelao, L., et al. (2007). Photocatalytic and antibacterial activity of TiO2 and Au/TiO2 nanosystems. *Nanotechnology, 18*(37), 1–7.

Chen, M., Zhang, E., & Zhang, L. (2016). Microstructure, mechanical properties, bio-corrosion properties and antibacterial properties of Ti-Ag sintered alloys. *Materials Science & Engineering. C, Materials for Biological Applications, 62*, 350–360.

Cheng, Q., Li, C., Pavlinek, V., Saha, P., & Wang, H. (2006). Surface-modified antibacterial TiO2/Ag+ nanoparticles: preparation and properties. *Applied Surface Science, 252*(12), 4154–4160.

Choi, H., Stathatos, E., & Dionysiou, D. D. (2006). Sol–gel preparation of mesoporous photocatalytic TiO2 films and TiO2/Al2O3 composite membranes for environmental applications. *Applied Catalysis B: Environmental, 63*(1–2), 60–67.

Damodar, R. A., You, S. J., & Chou, H. H. (2009). Study the self cleaning, antibacterial and photocatalytic properties of TiO2 entrapped PVDF membranes. *Journal of Hazardous Materials, 172*(2–3), 1321–1328.

Etacheri, V., Di Valentin, C., Schneider, J., Bahnemann, D., & Pillai, S. C. (2015). Visible-light activation of TiO2 photocatalysts: advances in theory and experiments. *Journal of Photochemistry and Photobiology C: Photochemistry Reviews, 25*, 1–29.

Goei, R., & Lim, T. T. (2014). Ag-decorated TiO2 photocatalytic membrane with hierarchical architecture: photocatalytic and anti-bacterial activities. *Water Research, 59*, 207–218.

Huo, K., Gao, B., Fu, J., Zhao, L., & Chu, P. K. (2014). Fabrication, modification, and biomedical applications of anodized TiO2 nanotube arrays. *RSC Advances, 4*(33), 17300–17324.

Lee, M. S., Hong, S.-S., & Mohseni, M. (2005). Synthesis of photocatalytic nanosized TiO2–Ag particles with sol–gel method using reduction agent. *Journal of Molecular Catalysis A: Chemical, 242*(1–2), 135–140.

Li, M., et al. (2011). Synergistic bactericidal activity of Ag-TiO(2) nanoparticles in both light and dark conditions. *Environmental Science & Technology, 45*(20), 8989–8995.

Li, H., Cui, Q., Feng, B., Wang, J., Lu, X., & Weng, J. (2013). Antibacterial activity of TiO2 nanotubes: influence of crystal phase, morphology and Ag deposition. *Applied Surface Science, 284*, 179–183.

Liu, Y., Wang, X., Yang, F., & Yang, X. (2008). Excellent antimicrobial properties of mesoporous anatase TiO2 and Ag/TiO2 composite films. *Microporous and Mesoporous Materials, 114*(1–3), 431–439.

Liu, F., et al. (2012). Nano-TiO2@Ag/PVC film with enhanced antibacterial activities and photocatalytic properties. *Applied Surface Science, 258*(10), 4667–4671.

Liu, L., Bai, H., Liu, J., & Sun, D. D. (2013). Multifunctional graphene oxide-TiO(2)-Ag nanocomposites for high performance water disinfection and decontamination under solar irradiation. *Journal of Hazardous Materials, 261*, 214–223.

Long, L., Xue, Y., Zeng, Y., Yang, K., & Lin, C. (2017). Synthesis, characterization and mechanism analysis of modified crayfish shell biochar possessed ZnO nanoparticles to remove trichloroacetic acid. *Journal of Cleaner Production, 166*, 1244–1252.

Ma, N., Fan, X., Quan, X., & Zhang, Y. (2009). Ag–TiO2/HAP/Al2O3 bioceramic composite membrane: fabrication, characterization and bactericidal activity. *Journal of Membrane Science, 336*(1–2), 109–117.

Macwan, D. P., Dave, P. N., & Chaturvedi, S. (2011). A review on nano-TiO2 sol–gel type syntheses and its applications. *Journal of Materials Science, 46*(11), 3669–3686.

Mai, L., Wang, D., Zhang, S., Xie, Y., Huang, C., & Zhang, Z. (2010). Synthesis and bactericidal ability of Ag/TiO2 composite films deposited on titanium plate. *Applied Surface Science, 257*(3), 974–978.

Morikawa, T., Irokawa, Y., & Ohwaki, T. (2006). Enhanced photocatalytic activity of TiO2−xNx loaded with copper ions under visible light irradiation. *Applied Catalysis A: General, 314*(1), 123–127.

Necula, B. S., Apachitei, I., Tichelaar, F. D., Fratila-Apachitei, L. E., & Duszczyk, J. (2011). An electron microscopical study on the growth of TiO2-Ag antibacterial coatings on Ti6Al7Nb biomedical alloy. *Acta Biomaterialia, 7*(6), 2751–2757.

Necula, B. S., van Leeuwen, J. P., Fratila-Apachitei, L. E., Zaat, S. A., Apachitei, I., & Duszczyk, J. (2012). In vitro cytotoxicity evaluation of porous TiO(2)-Ag antibacterial coatings for human fetal osteoblasts. *Acta Biomaterialia, 8*(11), 4191–4197.

Perkas, N., Lipovsky, A., Amirian, G., Nitzan, Y., & Gedanken, A. (2013). Biocidal properties of TiO2 powder modified with Ag nanoparticles. *Journal of Materials Chemistry B, 1*(39), 5309–5316.

Selvam, S., Rajiv Gandhi, R., Suresh, J., Gowri, S., Ravikumar, S., & Sundrarajan, M. (2012). Antibacterial effect of novel synthesized sulfated beta-cyclodextrin crosslinked cotton fabric and its improved antibacterial activities with ZnO, TiO2 and Ag nanoparticles coating. *International Journal of Pharmaceutics, 434*(1–2), 366–374.

Tan, S. X., Tan, S. Z., Chen, J. X., Liu, Y. L., & Yuan, D. S. (2009). Preparation and properties of antibacterial TiO2@C/Ag core-shell composite. *Science and Technology of Advanced Materials, 10*(4), 045002.

Tong, T., et al. (2013). Effects of material morphology on the phototoxicity of nano-TiO2 to bacteria. *Environmental Science & Technology, 47*(21), 12486–12495.

Wei, L., Wang, H., Wang, Z., Yu, M., & Chen, S. (2015). Preparation and long-term antibacterial activity of TiO2 nanotubes loaded with Ag nanoparticles and Ag ions. *RSC Advances, 5*(91), 74347–74352.

Yao, Y., Ohko, Y., Sekiguchi, Y., Fujishima, A., & Kubota, Y. (2008). Self-sterilization using silicone catheters coated with Ag and TiO2 nanocomposite thin film. *Journal of Biomedical Materials Research. Part B, Applied Biomaterials, 85*(2), 453–460.